MAGNETISATION AND ELECTRON SPIN RESONANCE STUDIES OF TETRAHEDRAL AMORPHOUS CARBON

M. M. Golzan[1], D. R. McKenzie[2], D. J. Miller[3], S. J. Collocott[4] and H. Hossein-Nejad[1]*

[1] *Department of Physics, Faculty of Science, University of Urmia, P. O. Box 165, Islamic Republic of Iran*
[2] *School of Physics, University of Sydney, NSW 2006, Australia*
[3] *School of Physics, University of New South Wales, NSW 2052, Australia*
[4] *CSIRO, Division of Applied Physics, P. O. Box 218, Lind field, NSW 2070, Australia*

Abstract

The magnetisation and electron spin resonance (ESR) spectrum of two specimens of tetrahedral amorphous carbon (ta-C), deposited from a filtered cathodic arc, were measured over a wide temperature range. The magnetisation was found to consist of superparamagnetic, paramagnetic and diamagnetic contributions. The superparamagnetic contribution resembled that recently found in carbon prepared from the tetrahedrally bonded substance adamantane. We found that the superparamagnetic contribution in ta-C correlated with low-level ferromagnetic contamination and that the properties were well described by the classical Langevin function with a temperature dependent magnetic moment. ESR measurements combined with the magnetisation results for the paramagnetic contribution gave consistent values of the electron spin density which showed a very high level unpaired electrons in ta-C. This high spin density shows that a large fraction of the residual sp^2 sites in ta-C are isolated in the sp^3 network.

Introduction

The intriguing possibility of strongly magnetic carbon materials has been raised in a recent work [1] in which the magnetic properties of a pyrolytic carbon prepared from adamantane were described as superparamagnetic or even ferromagnetic. The superparamagnetism was attributed to sp^3-type radicals in the residual structure of the adamantane. In this paper we report the magnetic properties of a highly tetrahedral amorphous carbon (ta-C) prepared by condensation of carbon plasma obtained from a cathodic arc operating in vacuum. This form of carbon has a fraction of sp^3 hybridised carbon of approximately 0.8 with the remainder being sp^2 hybridised [2,3]. Tetrahedral amorphous carbon is, with some important differences, structurally analogous to amorphous silicon and amorphous germanium. The differences are principally the presence of a considerable fraction of non-tetrahedral sites in ta-C and the greater rigidity of the tetrahedral bond angle in carbon than other group IV tetrahedral semiconductors. This bond angle stiffness is expressed by the high elastic stiffness of diamond

* *E-mail: m.golzan@urmia.ac.ir*

compared to other tetrahedral semiconductors, and may lead to requirement for the relatively large sp^2 concentration in order to relieve strain in the network[4,5].

The samples of ta-C were studied by measuring the magnetic susceptibility and the electron spin resonance (ESR) spectrum as a function of temperature. Like other adamantane materials, a strong superparamagnetic component was observed. There are some evidences that in the case of ta-C, this finding is due to traces of ferromagnetic impurities, originating from plasma duct of the preparation apparatus. The superparamagnetic behaviour was unusual since results at different temperatures did not superimpose when corrected for the temperature in the classical way.[6] In this respect the superparamagnetism was similar to that in dilute ferromagnetic alloys, for example, copper containing 2% of cobalt [7] and in fine particle dispersions. [8] There was also a strong paramagnetic contribution in the samples which could be explained in terms of sp^2 defects in the ta-C material. The system is therefore an interesting example of a dilute dispersion of superparamagnetic clusters in a paramagnetic matrix.

Experimental

Specimens of ta-C were prepared from high purity graphite (Ringsdorff, 99.995% carbon) in a filtered cathodic arc system fitted with a curved magnetic solenoidal filter of a type discussed previously [4]. The cathodic arc was struck in vacuum at 40-60 A current. This is a source of highly ionised carbon plasma and micrometre sized particles. The plasma is directed through the curved magnetic solenoid which traps the particles and gives a plasma beam consisting essentially of singly ionised carbon and electrons. The plasma beam is directed onto a fused silica substrate where it forms a deposit of ta-C which can be removed with a clean soft brush. The high compressive stress shown by ta-C causes it to peel spontaneously from most surfaces when its thickness increases beyond 100 nm or more.

A specimen containing trace levels of only ferromagnetic impurities and weighting 0.0567 g was prepared; this specimen was labelled as Specimen A. The trace ferromagnetic impurities come from stainless steel walls of the curved magnetic duct since some of the carbon ions collids with the walls and cause sputtering. The second specimen, Specimen B, was prepared by enrichment of the ^{13}C isotope with a much higher level of ferromagnetic impurities owing to the location of a stainless steel anode in front of the cathodic arc source. This specimen weighted 0.0117 g. The isotropic enrichment of this specimen has no effect on the interpretation of its magnetic properties. The compositional data for the two specimens are shown in Table 1 as determined by microanalysis. Measurements

of the magnetic moment were made at fields of up to 3.5 T in a Quantum Design Superconducting Quantum Interference Device magnetometer over the temperature range of 10 K to 350 K.

ESR spectra were recorded using a Bruker model ESP300 in the microwave X-band (9-10 GHz) over the temperature range of 100 K-300 K and a Varian ESR spectrometer at room temperature. The ta-C was diluted with high purity KCl powder to reduce the intensity of the absorption and to enable the entire length of the cavity to be filled. The spin density was determined by comparing the intensity with that of a standard sample of weak pitch in KCl, which also filled the entire length of the cavity, and with a diphenyl picryl hydrazyl standard.

Table 1. The composition of the impurities in parts per million in the two specimens of ta-C as determined by electron probe microanalysis

	Specimen A	Specimen B
Iron	50	4,750
Nickel	33	467
Cobalt	33	16
Chromium	17	683
Titanium	-	100
Manganese	-	333

Theoretical

Magnetic Susceptibility

The field dependence of the magnetisation per gram, M_p, in a paramagnet or superparamagnet may be written [9].

$$M_p = Ng\mu_B JB_J(y) \qquad (1)$$

where J is the total angular momentum quantum number (which we should assume to be due to electron spin only), g is the g-value of the electrons, N is the spin density (spins/g), μ_B is the Bohr magneton, y is the variable,

$$y = Jg\mu_B H / kT \qquad (2)$$

and $B_J(y)$ is the Brillouin function:

$$B_J(y) = [(2J+1)/2J] \coth[(2J+1)y/2J]$$

$$- (1/2J)\coth(y/2J). \qquad (3)$$

For a single electron spin, J = 1/2 and $B_J(y)$ reduces to the function

$$B_{1/2}(y) = \tanh(g\mu_B H / kT) \qquad (4)$$

For the case of superparamagnet, many spins in a cluster are aligned parallel to give a large J value so that the Langevin function L(y) may be used to approximate $B_J(y)$,

$$\lim_{J\to\infty} B_J(y) = \coth y - 1/y = L(y). \qquad (5)$$

Results
Magnetic Measurements

The results for the magnetisation as a function of the applied field for the specimen A are shown in Fig. 1 and for specimen B in Fig. 2.The data may be interpreted as a sum of three contributions to the magnetization

$$M(T,H) = N_1 g\mu_B J B_J(y) + C_1 H / (T+\theta) - C_2 H. \qquad (6)$$

The first term is a contribution of a form which is normally used to describe a superparamagnetic substance with spin clusters or domains with a spin quantum number $J.N_1$ is the number of such clusters in the specimen per gram. The second term describes a paramagnetic magnetisation arising from N_2 unpaired electron spins per gram with J =1/2. This term shows a Curie-Weiss behaviour with C_1 given by the Hund expression [9]

$$C_1 = (N_2 g^2 \mu^2_B) / 4k \qquad (7)$$

and θ is Curie temperature. The third term describes a diamagnetic contribution. Any graphite-related material in the sample would make a major contribution to this term since graphite is strongly diamagnetic parallel to its c-axis. The diamagnetism of graphite is temperature independent except above 200 K when the component parallel to the c-axis decreases [10] as T^{-1} and C_2 has been taken independent of temperature in this work.

Superparamagnetic Term

For superparamagnetic clusters with J >>1/2, the first component in Equation (6) is readily separated from the other two, since it saturates at relatively low fields. Therefore the coefficients of H in Equation (7) may be

found at each temperature by fitting a straight line to the high field behaviour. The first term, which is the superparamagnetic term, is then found from the intercept at H=0. The results for this term are shown in Figure 3 for Specimen A and in Figure 4 for Specimen B for temperatures below 150 K, the term linear in H was too large to enable the superparamagnetic to be evaluated reliably.

The magnetisation of a classical superparamagnet lies on a universal curve [6] when magnetisation is plotted against H/T. It is clear that the data in Figures 3 and 4 do not scale according to this relation and in fact the magnetisation versus H is nearly independent of temperature. The data do fit the Langevin function for a superparamagnetic substance in Equation (1) extremely well when the spin J on a cluster is allowed to vary with the temperature. The results of J with temperature is shown in Figure 5 which shows that J in both specimens has very similar behaviour despite the large difference in their ferromagnetic atomic concentrations. The variation of J in Figure 5 is required to maintain the essentially temperature independent magnetisation behaviour shown in Figures 3 and 4 and is consequently an approximately linear function of T.

In our data, the value of the saturation magnetisation of the superparamagnetic term correlates well with the concentration in atom percent of ferromagnetic atoms. Table 2 shows that the ratio of the saturation magnetisation of ferromagnetic spin clusters in the Specimen B to the Specimen A is 98.2. The ratio of iron impurity concentrations is 95.0, in good agreement, as described in Table 1.

Paramagnetic and diamagnetic Components

Once the superparamagnetic part of the magnetisation is removed, the paramagnetic component may be separated from the diamagnetic component by studying the temperature dependence of the magnetisation. The paramagnetic part is expected to obey a Curie-Weiss law whereas the diamagnetic component is expected to be temperature independent as discussed above.

Table 2. The parameters of the paramagnetic in the specimens from magnetic measurements

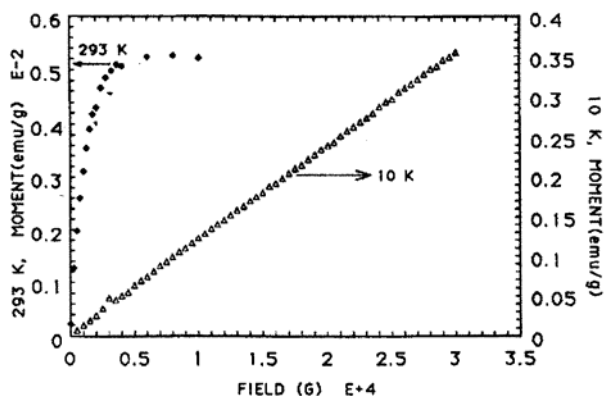| Quantity	Specimen A	Specimen B
M_s (emu/g)	5.5×10^{-3}	0.54
N_2 (spins/g)	1.9×10^{20}	2.0×10^{20}
θ (K)	4±3	6±3

Figure. 1. The magnetisation of the Specimen A expressed as the magnetisation per geram in emu as a function of applied magnetic field at 293 K and at 10 K.
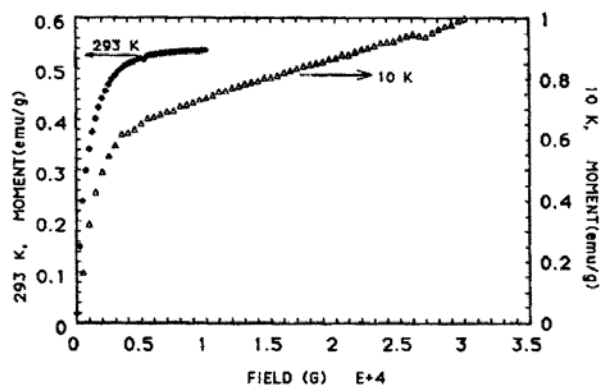

Figure. 2. The magnetisation as a function of applied magnetic field for the Specimen B at 293 K and at 10 K.
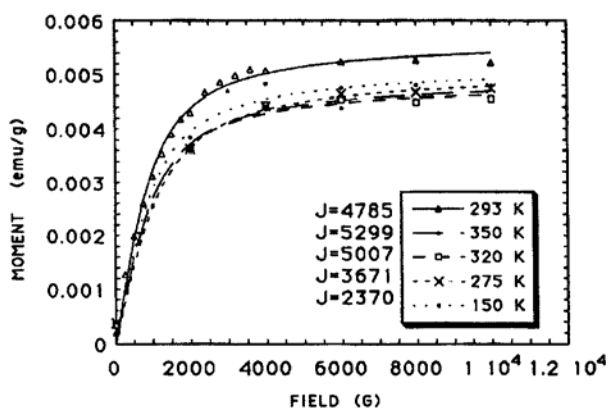

Figure. 3. The superparamagnetic contribution to the magnetisation of the Specimen A at various temperatures obtained by subtraction of the linear part of the magnetisation as discussed in the text. The theoretical curves are the best fits to the data using the Langevin function in Equation (5) with the values of J at temperature indicated on the diagram.

The values of the saturation magnetisation of the superparamagnetic clusters, M_s, and the concentration of the electron spins, N_2, and the Curie temperature, θ, of the paramagnetic contribution, were obtained from the best fits to the magnetisation as a function of field at various temperatures which are given in Table 2.

For the Specimen A, the reciprocal of paramagnetic of the total magnetisation at a constant field of 10^4 Gauss is shown as a function of temperature in Figure 6. The Curie-Weiss law is well obeyed by both specimens at low temperatures, giving Curie temperatures of 4±3K for the Specimen A and 7±3K for the Specimen B.

Finally, there was a strong diamagnetic contribution in each one of the samples and there was an evidence that the diamagnetic contribution increased with the age of the samples.

ESR Spectroscopy

The spectrum for the Specimen A is a single, relatively narrow line with a Lorentzian shape as shown in Figure 7 and has the properties summarised in Table 3. The g-value of 2.0022 is close to the free electron value consistent with the centers responsible for the spectrum being associated with carbon which has a low spin-orbit coupling constant. The spin density of 1.4×10^{20} spins per gram for the sample A is in reasonable agreement with fashion magnetically determined values for the concentration of paramagnetic centers given in Table 2 and this suggests that the same centers are responsible for both the ESR signal and the strong paramagnetism in the sample.

The intensity of the absorption increases with decreasing temperature in a Curie-Weiss law fashion:

$$I = C' / (T + \theta') \tag{8}$$

where I is the intensity of the absorption at temperature T. Figure 8 shows the reciprocal of I plotted as a function of temperature for the Specimen A. The reciprocal of the intensity deviates from the Curie-Weiss law at higher temperatures. The points corresponding to the three lowest temperatures may be fitted with a straight line according to Equation (8), giving a value of θ' of 10±4 K (see Table 3). This value of θ' is in agreement with the value determined from magnetic susceptibility measurements. The line width remained constant with temperature in the range 100 K - 293 K as shown in Figure 9 and the signal showed no saturation with microwave power up to 1 mW which the signal begins to saturate after it, as shown in Figure 10.

The ESR signal from the Fe-enriched specimen B is compared with that of the Specimen A in Figure 7 and the relevant parameters are compared in Table 3. The main differences are the linewidth of Specimen B is
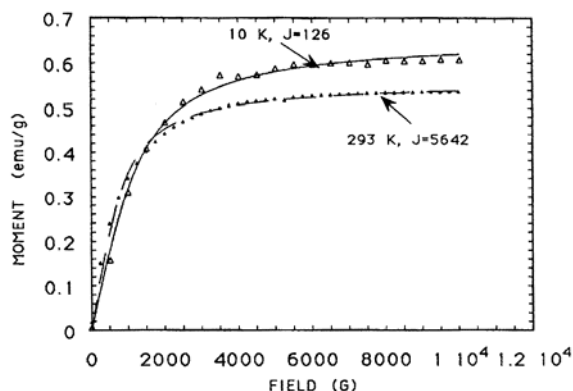
Figure. 4. The superparamagnetic contribution to the magnetisation of the Specimen B at 293 K and 10 K obtained as for the Specimen A.
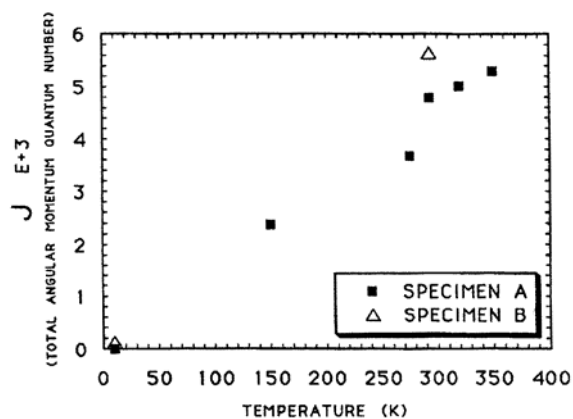

Figure. 5. The value of the spin quantum number **J** for superparamagnetic spin clusters obtained by fitting relation (1) to the magnetisation data at various temperatures.
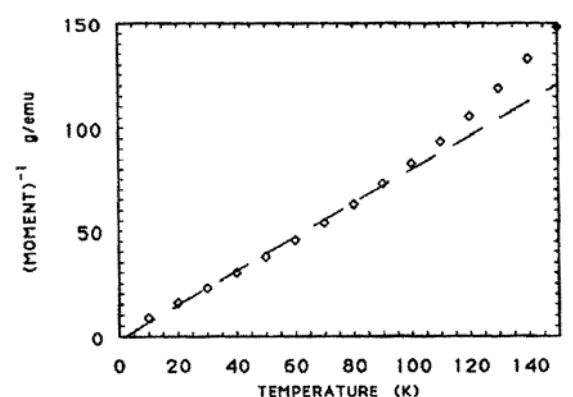

Figure. 6. The reciprocal of the paramagnetic part of the magnetisation of the Specimen A at 10^4 Gauss as a function of temperature. The Curie-Weiss relation is well obeyed at low temperatures.

Table 3. The parameters of the ESR signals in the specimens

Parameter	Specimen A	Specimen B
Spin Density (spins/g)	1.4×10^{20}	1.3×10^{20}
g-value	2.0022	1.998± 0.0003
Line Width (Gauss, 293 K)	3.4	40.0
Curie Temperature (K)	10±4	-28±10

about an order of magnitude larger and is temperature dependent, with a lineshape which is slightly broader than Lorentzian in the wings. The saturation of the ESR signal occurs at higher microwave power levels than in the Specimen A as shown in Figure 10. Also the g-value has been reduced slightly below the free electron value in the Specimen B. However, the Specimen B has the same spin density as the Specimen A, as shown in Table 3. The data obtained from the Specimen B deviates somewhat from a Cuie-Weiss law as shown in Figure 8. The Curie temperature determined from extrapolation of the lowest temperature data is closer to 0 K than the Curie temperature obtained by extrapolations which include the high temperature data that lead to a Curie temperature of −28±10 K. The deviations from the Curie-Weiss law are discussed further below and more measurements would need to be made to establish whether the Curie temperatures of the different samples determined from ESR are significantly different.

Discussion and Results

There are three separate contributions to the magnetic properties of ta-C: a diamagnetic contribution, a superparamagnetic contribution and a paramagnetic contribution. Within experimental error, the same spin densities were obtained from the paramagnetic component of the magnetic susceptibility at low temperature and from the ESR for both the Specimen A and the Specimen B. Thus it is very likely that the same unpaired spins contribute to the ESR signal as give rise to the paramagnetic moment and that the unpaired spin density is unaffected by the concentration of Fe.

A schematic density of states diagram of ta-C is shown in Figure 11. The most important feature of this diagram for the magnetic and ESR properties are the normally occupied π states below the Fermi energy and the lowest lying unoccupied π* states above the Fermi energy. The π states are associated with sp^2 sites and account for the electrical conductivity of the ta-C through a hopping mechanism. Electron energy loss spectroscopy shows [2] that approximately 20% of carbon sites in ta-C are sp^2 leading to a density of π states of 1×10^{22} spins per gram. We suggest that the normal paramagnetism and ESR signal reported in this work are due to unpaired electrons in the π states of isolated sp^2 sites. The wave functions associated with
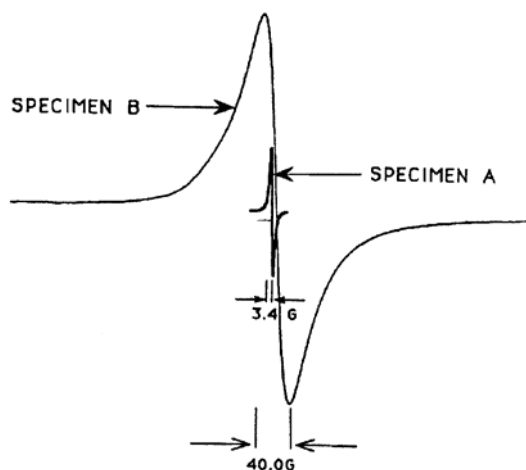
Figure. 7. The first derivative of the electron spin resonance absorption in the Specimen A (small narrow signal) compared with that of the Specimen B (large broad signal).
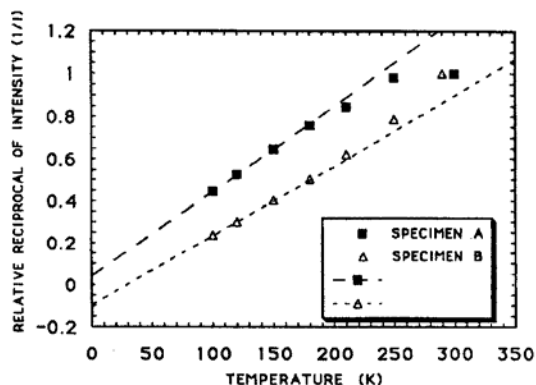

Figure. 8. The recipared of the ESR signal intensity for the Specimen A (solid symbols) and the Specimen B (hollow symbols) in arbitrary units as a function of temperature. Except for temperatures above room temperature a Curie-Weiss law is obeyed approximately.
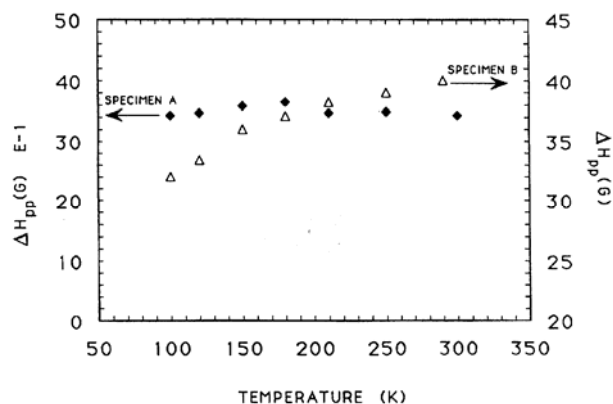

Figure. 9. The linewidth of the ESR signals of the Specimen A and the Specimen B as a function of temperature.

these states are likely to be localised in view of their random distribution in the network, forming a type of defective site. The measured density of paramagnetic centers is about 2×10^{20} spins per gram and this indicates that 2% of sp^2 sites have an unpaired spin associated with them. This could occur either through a partial occupancy of the sp^2 sites all of which are of the isolated, singly-occupiable type or if the majority of the sp^2 sites are paired with only about 2% of the sites isolated and occupied by unpaired electrons. The latter alternative could occur if the majority of the sp^2 sites are adjacent to the another and the electrons on each site pair up. In the former case, the sites could be partially occupied owing to thermal excitation to the π^* states or the extended stated shown in Figure 11 but in this case, one would expect the unpaired spin density change with temperature. No temperature dependence is observed except that the spin density measured by ESR in the sample A drops off at temperatures above 250 K.

A similar decrease in spin density would be expected to be observed in the magnetic susceptibility data but the paramagnetic contribution is masked at high temperatures by the other contributions and this could not be confirmed. It is probable then that the observed decrease in the spin density above 250 K is due to a change in the occupancy of the sites, perhaps due to a shift in the Fermi level in the Specimen A which dose not occur in specimen B where no reduction in the spin density is observed. Since the spin density is independent of temperature except for this case, we conclude that the second mechanism applies and the majority of sp^2 sites do not show spin because of electron pairing with neighbouring sites. The pairing of spins on neighbouring sp^2 sites would not be detected in the electron spectroscopy measurements [2] which are only sensitive to the density of electron states and not to spin. The diamagnetic component of the magnetisation could be due to either the paired π states described above or presence of small quantities of graphite-related materials which produce a measurable effect because graphite is strongly diamagnetic. The unusual feature of the superparamagnetic component was that it could not be explained by the universal expression [6] in Equation (3) which scales with H/T at different temperatures T. The electron spins in the superparamagnetic cluster are combined to give a large magnetic moment J but the cluster will only contribute to the magnetic properties of the sample if the cluster is able to reverse its magnetic moment on the measurement timescale. In a solid matrix, bulk rotation of the single domain clusters is ruled out, as discussed by Bean and Livingston [6]. The clusters can change their direction of magnetisation only in a case of Brownian motion, as originally discussed by Neel [11]. Large clusters cannot change their direction
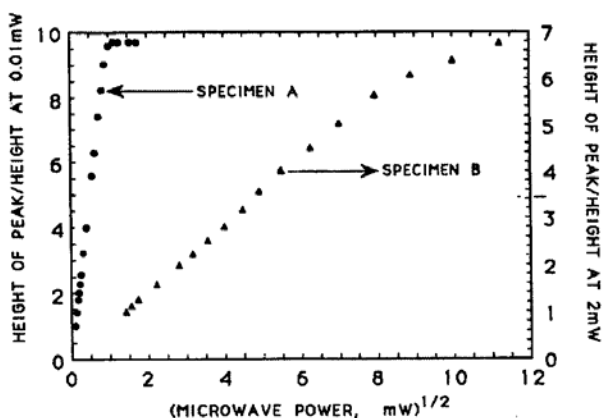
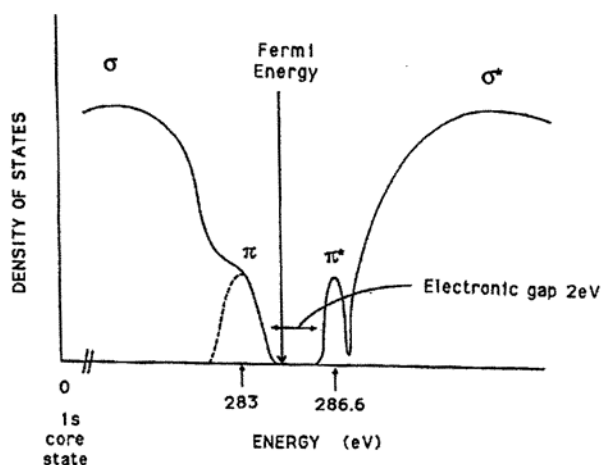**Figure. 10**. The ESR signal intensity of the specimens as function of microwave power showing the saturation.

Figure. 11. A schematic diagram of the density of states for ta-C showing the states labelled π and π^* arising from sp^2 bonded atoms and states labelled σ and σ^* arising from sp^2 and sp^3 bonded atoms.

until a sufficiently large relaxation time has elapsed which decreases with increasing temperature. Therefore, as the temperature increases, the size of the clusters which can participate in the magnetic response on the 'time scale of the experiment also increases, leading to a larger average J of the contributing clusters as shown in Figure 5. Weil [7] observed a similar phenomenon in a copper alloy containing 2% of cobalt and showed that heavy deformation modified the cluster size distribution. This type of behaviour has also been reported from superparamagnetic particles in a frozen fluid [8].

The ESR results show that the larger concentration of the superparamagnetic clusters in the relatively Fe-rich specimen B causes an increase in the linewidth and a decrease in the g-value of the signal. The increase in the linewidth of the signal is probably due to the internal magnetic field of the superparamagnetic clusters leading to inhomogeneous broadening of the ESR spectrum from the unpaired spins which are distributed at different distances from the superparamagnetic clusters. In the Specimen A, there are far fewer superparamagnetic clusters and most of the sp^2 sites are far from any cluster so that less broadening is observed. The results from the present samples are similar to those from pyrolytic carbon prepared from vaporised adamantane [1] in which there is a diamagnetic contribution, a strong paramagnetic contribution, with accompanying ESR signal, and a strong superparamagnetic contribution to the magnetisation. The narrow component of the ESR signal in the adamantane samples was attributed [1] to π-type spins occurring in a frustrated sp^2-carbon network which is similar to the explanation or the ESR signal in the ta-C samples studied here. However, unlike the present results, the superparamagnetic behaviour in the adamantane sample was considered to be intrinsic and to sp^3-type radicals (σ-spins) remaining in the product structure since it appeared that there was insufficient Fe or other ferromagnetic impurities in the adamantane samples [1]. In our ta-C samples, the superparamagnetic component correlates well with the Fe content and therefore there is no evidence of the intrinsic collective magnetic effects reported in the adamantane samples. The present magnetic results have implications for the electronic properties of ta-C. It is known that there is a large concentration of sp^2-sites in ta-C and the present magnetic measurements show that a significant fraction of these sites are occupied by unpaired electrons because the sites are isolated. Since ta-C shows photoconductivity [13] and is capable of accepting n-type dopants [14,15] the unpaired electron do not act as recombination centers as do the dangling bond sites in amorphous Si for example. In fact the number density of the π states is sufficiently large that they make a major contribution to the density of states and hence are involved in the conduction process itself.

References

1. Tanaka, K., Kobashi, M., Sanekata, H., Takata, A., Yamabe, Y., Mizogami, S., Kawabata, K. and Yamauchi, L. J. *J. Appl. Phys.,* **71**: 836 (1992).
2. Berger, S. D., McKenzie, D. R. and Martin, P. J. *Phil. Mag.* **57**: 285 (1988).
3. Gaskell, P. H., Saeed, A., Chieux, P. and McKenzie, D. R. *Phys. Rev. Lett.* **67**: 1286 (1991).
4. McKenzie, D. R., Muller, D. A. and Pailthorpe, B. A. *Ibid.,* **67**: 773 (1991).
5. Golzan, M. M., Lukins, P. B., Mckenzie, D. R., Vassallo, A. M. and Hanna, J. V. *J. Phys. Chem.,* **193**: 167-72, (1995).

6. Bean C. P. and Livingston, J. D. *J. Appl. Phys.,* Suppl. to Vol. **30**: 120S, (1959).

7. Weil, L. *J. Phys. Radium,* **20**: 282, (1959).

8. Williams, H. D., O'Grady, K., Hilo, M. EI and Chantrell, R. W. *J. Magn. Magn. Mater*, **122**: 129, (1993).

9. Morrish, A. H. *The Physical Principles of Magnetism.* Wiley, New York, p. 71, (1965).

10. Brandt, N. B., Chudinov, S. M. and Ponomarev, Y. G. *Semimetals I: Graphite and its Compounds,* Vol. 20.1 of Modern Problems in Condensed Matter Sciences, North Holland, Amsterdam, p. 175, (1988).

11. Neel, L. *Compt. Rend,* **228**: 664 (1949).

12. Linderoth, S., Balcells, L., Labarta, A., Tejada, T., Hendriksen, P. V. and Sethi, S. A. *J. Magn. Magn. Mater,* **124**: 269, (1993).

13. Amaratunga, G. A. J., Veerasamy, V. S., Milne, W. I., Davis, C. A., Silva, S. R. P. and McKenzie, D. R. *Appl. Phys. Lett.,* **63**: 370, (1993).

14. Veerasamy, V. S., Amaratunga, G. A. J., Davis, C. A., Timbs, A. E., Milne, W. T. and McKenzie, D. R. *J. Phys. Cond. Matter,* **5**: 2169, (1993).

15. McKenzie, D. R., Yin, Y., Marks, N. A., Davis, C. A., Kravtchinskaia, E., Pailthorpe, B. A. and Amaratunga, G. A. J. *J. Non-Crystalline Solids,* **164-166**: 1101, (1993).